

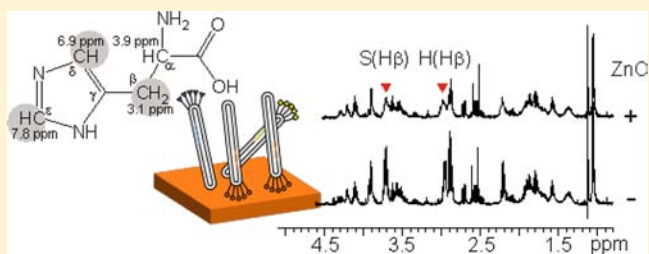
Isolation of ZnO-Binding 12-mer Peptides and Determination of Their Binding Epitopes by NMR Spectroscopy

Dirk Rothenstein,^{*,‡} Birgit Claasen,[§] Beatrice Omiecinski,^{‡,†} Patricia Lammel,[‡] and Joachim Bill[‡]

[‡]Institute for Materials Science and [§]Institute for Organic Chemistry, University of Stuttgart, 70569 Stuttgart, Germany

S Supporting Information

ABSTRACT: Inorganic-binding peptides are in the focus of research fields such as materials science, nanotechnology, and biotechnology. Applications concern surface functionalization by the specific coupling to inorganic target substrates, the binding of soluble molecules for sensing applications, or biomineralization approaches for the controlled formation of inorganic materials. The specific molecular recognition of inorganic surfaces by peptides is of major importance for such applications. Zinc oxide (ZnO) is an important semiconductor material which is applied in various devices. In this study the molecular fundamentals for a ZnO-binding epitope was determined. 12-mer peptides, which specifically bind to the zinc- or/and the oxygen-terminated sides of single-crystalline ZnO (0001) and (000-1) substrates, were selected from a random peptide library using the phage display technique. For two ZnO-binding peptides the mandatory amino acid residues, which are of crucial importance for the specific binding were determined with a label-free nuclear magnetic resonance (NMR) approach. NMR spectroscopy allows the identification of pH dependent interaction sites on the atomic level of 12-mer peptides and ZnO nanoparticles. Here, ionic and polar interaction forces were determined. For the oxygen-terminated side the consensus peptide-binding sequence (HSXXH) was predicted *in silico* and confirmed by the NMR approach.



INTRODUCTION

Peptides, which bind to inorganic technical materials, possess great importance for the fabrication of devices like sensors,^{1,2} and applications like surface functionalization,³ imaging,⁴ or biomineralization.⁵ The biochemical versatility of peptides, which originates from the sequential combination of about 20 different genetically encoded amino acid building blocks, makes them ideal candidates for highly specific interactions. The peptide properties can be modified by the alteration of the amino acid sequences, leading to tailored molecules for bottom-up approaches to generate nanostructured materials. In particular, the molecular recognition and self-assembly functionalities of peptides make them effective tools.

Bioinspired mineralization processes, which aim at the formation of multifunctional organic–inorganic hybrid materials, have been applied for the generation of ZnO nanostructures. ZnO exhibit piezoelectric properties and is an important and widely applied semiconductor.⁶ Empirically established results show, that single amino acids, dipeptides, and proteins influence the mineralization of ZnO from appropriate precursor solutions under soft reaction conditions. Thereby, the morphology^{7,8} and the crystallinity⁹ of the synthesized ZnO can be controlled. Inorganic-binding peptides have been identified from random peptide libraries using screening methods like phage display (PD) or cell surface display (CSD). With those approaches peptides, which specifically interact with oxides like ZnO,^{10–13} SiO₂,¹⁴ TiO₂,¹⁵ metals like Au,¹⁶ Ag,¹⁷ Pd,¹⁸ and semiconductors like ZnS,¹⁹ and CdS,²⁰

were isolated. The PD system was applied for systematic investigations using ZnO powder as target substrate. Only CSD experiments applied single-crystalline ZnO as binding substrate; however the crystallographic plane of the substrate was not specified.¹⁰

Peptide based binding epitopes for inorganic target materials were difficult to assign, because of the heterogeneity of the isolated peptide sequences. The enrichment and the depletion of amino acids in those peptide pools provide first insight into which amino acids may account for the binding to inorganic materials. The interactions of single amino acid residues to ZnO have been investigated.^{21–23} However, the molecular basis of the organic–inorganic interactions is not entirely understood. It was supposed, that chemical and physical effects contribute to the binding strength of a peptide to an inorganic material.²⁴ Ionic interactions of charged atoms are one of the major driving forces in addition to polar interactions of uncharged atoms, like hydrogen bonds, van der Waals forces, and hydrophobic effects. The molecular basis of the substrate recognition and binding remains ambiguous and therefore a rational peptide design for the binding to an inorganic material of interest is not yet achieved.

During the past two decades nuclear magnetic resonance (NMR) spectroscopy in solution has gained significant importance since sensitivity and resolution of the NMR

Received: March 6, 2012

Published: June 21, 2012

spectrometers have improved dramatically and new methods have been described. Several NMR spectroscopic parameters may serve as a gauge for the detection and analysis of binding events in solution. Among these, chemical shift perturbations and line-broadening effects upon target binding are often used to detect interactions and to characterize binding epitopes in bioorganic molecules on an atomic level. In contrast to many other binding assays, NMR spectroscopy is a label-free analysis method, avoiding changes in charge distribution and conformation of the peptide, which might influence the binding.

This study aims at the identification of ionic and nonionic (polar) interactions of peptides with inorganic ZnO substrates to reveal the molecular basis of the substrate recognition and binding. So far, no direct analysis method has been described in order to provide information about the binding sites of inorganic-binding peptides on the atomic level. Inorganic binding peptides for the surface terminations (0001) and (000-1) of single-crystalline ZnO target substrate were identified by PD experiments. The two most abundant peptides were further analyzed by NMR spectroscopy to determine ZnO-binding epitopes, i.e. the amino acid residues which contribute to the binding of the peptides to ZnO. In addition, the pH dependency of the binding was determined.

METHODS

Phage Display. Zinc oxide binding peptides were isolated from a random 12-mer peptide library (New England Biolabs, Inc.) using PD technique. The DNA sequences of the 12-mer peptides from the combinatorial peptide library are N-terminal fused to the gIII of the bacteriophage M13. The peptides are separated by a short spacer sequence (GGGS) from the pIII major coat protein. The peptide library consists of approximately 2.7×10^9 different peptides each present in 55 copies in 10 μ L of phage solution. General phage methods were conducted according to the manufacturer's recommendations.

Single-crystalline ZnO (0001) and (000-1) substrates were used for PD experiments as received by the manufacturer (CrysTec, Berlin, Germany). The biopanning procedure was conducted using the zinc- or the oxygen-terminated side of the substrate, respectively. Therefore, one side of the polar target substrate was blocked in the experimental setup with Teflon tape. The target substrate was washed twice with Tris buffered saline (TBS), pH 7.5 supplemented with 0.1% Tween 20. The random phage library (1.5×10^{11} phages) was challenged to the ZnO substrate under light agitation in TBS, 0.1% Tween20 for one hour at RT. Unbound and weakly bound phages were removed from the substrate by washing 10 times with TBS, 0.5% Tween 20. The remaining phages were eluted applying ultrasound for 5 min (Sonorex RK 52H, Bandelin). The obtained phages were amplified in *E. coli* ER2738, and purified by polyethylene glycol-8000/sodium chloride (PEG/NaCl) precipitation with subsequent centrifugation steps. In following bio panning rounds at least 1.3×10^{10} phages were applied. To enrich the peptide pool for ZnO-binding sequences, in total 3 panning rounds were carried out. The experiments were done in triplicate and from each experiment 30 randomly selected phage clones were analyzed by DNA sequencing.

Binding Strength Assay. To evaluate the binding strength of a single peptide sequence, a phage clone expressing one peptide sequence only was amplified according to manufacturer's recommendations. Briefly, an *E. coli* ER2738 overnight culture was diluted 1:100 in Lysogeny broth (LB) medium and inoculated with 3 μ L phage suspension. The culture was incubated at 37 °C; 250 rounds per minute (rpm) for 4.5 h. Bacterial cells were removed by centrifugation (10 min; 4500 g). Phages in the upper 80% of the solution were precipitated adding 2.5 M NaCl/20% PEG-8000 to a final volume of 20%. Phages were pelleted by centrifugation (15 min; 12000 g), resuspended and precipitated a second time to obtain higher purity. Finally phages were suspended in TBS, (50 mM Tris pH 7.5; 150 mM

NaCl). The phage titer was determined in three independent experiments.

A defined amount of identical phages, expressing only one peptide, or M13 wt phage, as negative control, were bound to single-crystalline ZnO in TBS at RT for 1 h. The zinc- or the oxygen-terminated side of the target substrate was blocked using Teflon tape, respectively. Unbound phages were excluded by 5 washing steps each applying TBS supplemented with 0.5% Tween 20. Bound phages were eluted by ultrasound (5 min in TBS supplemented with 0.5% Tween 20). The phage titer (number of bound phages) was determined according to manufacturer's recommendations using appropriate dilutions of the eluted phages. The phage titer directly correlates with the binding strength of a single clone. The phage titers were normalized to wt phage titers (wt phage titer = 1).

Electrokinetic Measurements. Electrokinetic measurements on single-crystalline ZnO were conducted using the SurPASS electrokinetic analyzer (Anton Paar, Graz, Austria). Epipolished ZnO (0001) and (000-1) substrates with a dimension of 10 \times 10 mm and a thickness of 0.5 mm, an orientation tolerance of $<0.5^\circ$ (typically $<0.3^\circ$), and a root-mean-square roughness of 0.191 nm for the zinc-terminated and 0.162 nm for the oxygen-terminated side were applied in the experiments. The substrates were washed according to Rabung et al.²⁵ Briefly, the substrates were incubated in acetone overnight, and then washed with ethanol for 2 h, and finally washed several times in ddH₂O. The zeta potential (ZP) was determined by streaming current measurements in an adjustable gap cell with rectangular streaming channel geometry and a 100 μ m gap between the substrates. Streaming current experiments were conducted in 1 mM and 10 mM NaCl or KCl electrolyte solution. The pH value of the electrolyte solution was titrated from basic to acidic pH values using the automatic titration unit.

Nuclear Magnetic Resonance Measurements. NMR spectra were recorded at 296 K at a Bruker Avance 500 spectrometer equipped with a 5 mm BBO probe head. Standard 5 mm NMR-tubes were used (Wilmad). NMR samples of peptide 31 and 44 (1.5 mg/mL) were prepared in 50 mM phosphate or acetate buffer in H₂O:D₂O (9:1) and the pH was adjusted to 4.0, 5.0, 6.0, 7.0, 7.5, or 8.0, respectively. ZnO nanoparticles (20 nm particle size, IoLiTec Ionic Liquids Technologies GmbH, Germany) were suspended in H₂O and centrifuged afterward. The supernatant, containing non-agglomerated nanoparticles was added (150 μ L). For ZnO titration experiments samples were prepared in 50 mM phosphate buffer in H₂O:D₂O (9:1) at pH 7.5 with a peptide concentration of 1.1 mM (1.5 mg/mL). One-dimensional spectra were recorded with 32k data points and a repetition delay of 2 s. Two-dimensional spectra were acquired with 2k-4k data points in t₂ and 256 increments in t₁. ROESY spectra were recorded with a mixing time of 300 ms and TOCSY-spectra were run with a spin-lock time of 120 ms. Water suppression was achieved by the application of the WATERGATE w5-sequence. Spectra processing was performed using Topspin 1.3 software (Bruker Biospin). Processing parameters: $\pi/2$ shifted sine² (QSINE, SSB 2) apodization was applied in both dimensions prior to Fourier transformation. The NMR assignment of the peptide resonances of peptide 31 and 44 at pH 4 is summarized in the Supporting Information.

RESULTS

Isolation of Peptide Sequence. A random 12-mer peptide library expressed as fusion protein to the minor coat protein pIII of M13 phages was challenged for the binding to the zinc-terminated/(0001) or the oxygen-terminated/(000-1) side of hexagonal single-crystalline ZnO. In total 82 peptides were isolated showing 29 different peptide sequences (Table 1). Ten peptides bound only to the oxygen-terminated side of the substrate. For the zinc-terminated side, 13 interacting peptides were identified. Six peptides were isolated from both, the oxygen- and the zinc-terminated side of the ZnO substrate, among these were the peptide 44 (HSSHQPKGTNP) and

Table 1. Peptides Binding to Zinc Oxide Single-Crystalline Substrate in the (0001) Orientation

peptide ^a	frequency	sequence ^b	substrate ^c	pI ^d
06	1/82	QWGNMPLVEAQ	O	4.00
46	1/82	ERSWTLDLSALSM	Zn	4.37
83	1/82	SNNDLSPLQTSH	Zn	5.08
21	1/82	DSSNPIFWRPSS	Zn	5.84
19	1/82	SILSTMSPHGAT	Zn	6.74
26	1/82	SHALPLTWSTAA	Zn	6.74
07	5/82	LLADTTHHRPWT	O/Zn	6.92
24	1/82	HSHLHHSIQQA	O	7.10
32	1/82	HVSIHRTTHHEM	Zn	7.10
52	1/82	MKPKAIRLDLL	Zn	8.59
23	1/82	HYPTAKFHAERL	Zn	8.60
20	1/82	TKNMLSLPVGPG	Zn	8.75
22	1/82	FNTGSQMHQKFP	Zn	8.76
12	1/82	NHVHRMHATPAY	O	8.77
44	25/82	HSSHHQPKGTNP	O/Zn	8.77
15	1/82	HYQHNTHHPSRW	O	8.78
53	1/82	HHTHRVDVHQTR	Zn	9.62
29	1/82	FGLTAPRSASIL	Zn	9.75
58	1/82	APRLPQSLLPQL	Zn	9.75
09	1/82	HSSPHFSRTWAS	O	9.76
36	1/82	HHRTLSPSVSIL	O	9.76
03	5/82	HSSPHFSRHGLL	O	9.77
31	17/82	HHGHSPTSPQVR	O/Zn	9.77
05	2/82	NTIHHRRHMPPP	O	9.78
43	2/82	SHNHPPRHTAHS	O/Zn	9.78
70	1/82	SSGLRHSQQHP	O	9.78
25	3/82	HSKLNRRHALL	O/Zn	11.00
45	2/82	HTKPHHTPTQRA	O/Zn	11.00
38	1/82	GHIHSRHRPPT	O	12.00

^aIn total 29 peptide sequences were obtained from 90 analyzed phage clones. Eight phage clones did not harbor an additional peptide sequence. ^bThe amino acids of the peptide sequence are denoted in single letter abbreviations. ^cThe substrate orientation specifies if the peptides were isolated from the zinc (Zn)-, or/and oxygen (O)-terminated side of the polar substrate. ^dPeptide sequences are sorted by the calculated isoelectric point (pI) (Vector NTI software, Invitrogen).

peptide 31 (HHGHSPTSPQVR). While most of the sequences were isolated only once, peptide 44 and peptide 31 were isolated 25 and 17 times, respectively.

Analysis of Peptides. The amino acid residue frequency of the isolated ZnO-binding peptides was altered in comparison to the naïve peptide library. The percentage of the occurrence of amino acid residues in the isolated peptide pools for the oxygen- and the zinc-terminated sides of the substrates compared to the unchallenged peptide library were calculated (Table 2). Amino acids deviating more than 25% from the observed frequency in the naïve peptide library were considered as enriched or depleted, respectively.

The basic amino acid histidine (H) was enriched for the oxygen- and the zinc-terminated substrate sides. In addition, for the oxygen-terminated side arginine (R) and for the zinc-terminated side lysine (K) was enriched. Noteworthy, amino acid residues enriched in peptides, which were isolated from the zinc-terminated ZnO (K, D, L, and A) were depleted in peptides isolated from the oxygen-terminated side. Negatively charged amino acid residues were completely depleted in the peptide pool isolated from the oxygen-terminated side. Interestingly, from the zinc-terminated side, only the frequency

Table 2. Amino Acid Frequency of the Isolated ZnO-Binding Peptides^A

Zn-terminated side		O-terminated side	
amino acid	multiplication factor	amino acid	multiplication factor
G	1.48	H	3.97
H	1.42	R	1.66
S	1.41	G	1.20
K	1.37	S	1.20
D	1.37	W	1.18
L	1.31	M	1.00
A	1.28	N	0.91
M	1.23	P	0.90
I	1.13	T	0.80
R	1.09	Q	0.71
F	0.97	A	0.69
Q	0.88	V	0.67
W	0.87	I	0.61
P	0.74	L	0.56
N	0.70	K	0.56
T	0.69	F	0.32
V	0.49	Y	0.29
E	0.20	D	0.19
Y	0.18	E	0.17
C	0.00	C	0.00

^AThe frequency of amino acid residues in the isolated peptides compared to the frequency of the naïve peptide library (New England Biolabs). The multiplication factor specifies the frequency of amino acid residues observed and expected. Amino acids were grouped in high abundance (multiplication factor higher than 1.25), similar frequency (multiplication factor in between 0.75 to 1.25), and low frequency (multiplication factor less than 0.75).

of the negatively charged glutamic acid (E) was depleted while the frequency of the also negatively charged aspartic acid (D) was enriched, indicating that ionic interactions are not the only forces which can be accounted for the peptide-inorganic binding.

The values of the calculated isoelectric points (pI) of ZnO-binding peptides (Vector NTI software, Invitrogen) range from 4.00 to 12.00; 69% of the peptide sequences show $pI \geq 7.5$, while only 31% of the sequences have $pI \leq 7.5$. The peptides were grouped into three categories according to their calculated pI: acidic (pH 3.0–5.9), neutral (6.0–8.9), and basic (9.0–12.0), respectively (Figure 1). The percentages of peptides with acidic and neutral pI were increased for the zinc-terminated side compared to peptides binding to the oxygen-terminated side, which show an increase for the basic pI. This correlates with the determined ZPs of the oxygen- and the zinc-terminated single-crystalline ZnO substrate (Figure 2). The ZP of oxygen-terminated ZnO is more negative than that of the zinc-terminated side.

Binding Assay. In order to determine the binding strength of individual phage clones to ZnO the phage clones expressing either peptide 44 or peptide 31 were bound to zinc- and oxygen-terminated single-crystalline ZnO (0001), respectively.

To normalize the binding strength the titer of bound wild-type (wt) M13 phages was used (Figure 3). In general, the binding to the oxygen-terminated substrate side was more efficient than to the zinc-terminated side. Peptide 31 showed the highest binding strength for both ZnO sides. For the zinc-terminated substrate side the binding strength for the phage clone 31 and 44 increased by the factor of 3.13 and 2.54,

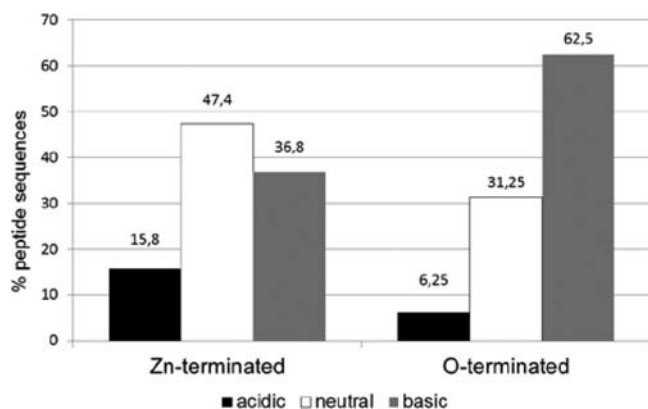


Figure 1. Distribution of the isoelectric points (pI) of ZnO-binding peptides isolated from zinc (Zn)- or oxygen (O)-terminated ZnO crystal substrates. The pI range was split into three groups: acidic (pH 3.0–5.9), neutral (pH 6.0–8.9), and basic (pH 9.0–12.0) and the percentages of ZnO-binding peptides were plotted according to their calculated pI .

respectively. The binding strength for the oxygen-terminated side increased 8.43-fold for phage clone 31 and by the factor of 4.43 for the phage clone 44.

Sequence Alignment. Almost 80% of the ZnO-binding peptides contained at least one histidine residue. The analysis of the isolated peptide sequences from the zinc- and the oxygen-terminated substrate sides showed that 12 out of the 29 peptides (41.4%) contained a histidine-histidine (HH) dipeptide motif within their sequences (Figure 4A).

The putative binding motive HSXXH of peptides binding to the oxygen-terminated side of the substrate was identified based on conserved amino acid residues (Figure 4B). The putative binding motive was found in approximately one-third of the sequences. For peptides from the zinc-terminated substrate side an increased frequency of leucine (L) neighboring a polar, uncharged amino acid residue (serine (S) or threonine (T)) was identified.

Nuclear Magnetic Resonance Measurements. The binding epitope of ZnO on peptides 31 and 44 was investigated by analysis of the NMR chemical shift perturbations and line-

broadening effects upon ZnO binding. Therefore, peptide resonances were assigned with standard 2D NMR experiments (see Supporting Information for TOCSY and ROESY spectra). For the latter experiments the pH was adjusted to pH 4 in order to visualize the exchangeable NH protons of the peptide backbone.

1D ^1H NMR spectra of peptides 44 and 31 were acquired in presence and absence of ZnO nanoparticles at pH 4.0, 5.0, 6.0, 7.0, 7.5, and 8.0. The results show that the interaction between peptide 44 and ZnO is strongly pH-dependent. Comparison of the 1D ^1H NMR spectra of peptide 44 in the presence and absence of ZnO at pH 4 clearly reveals that only the $H_{\epsilon 1}$ proton of the histidine residue at position one of the peptide sequence (H1) is affected by the binding, while additional significant line-broadening effects are observed for the $H_{\epsilon 1}$, $H_{\delta 2}$ and H_{β} protons of all histidine residues and the H_{β} protons of the serine residues at pH 7.5 (Figure 5A).

Interestingly, peptide 31 does not show any significant line-broadening effect at pH 4.0 and only the $H_{\epsilon 1}$ proton from one of the three histidine residues is broadened at pH 7.5 upon ZnO binding (Figure 5B).

The side chain protons of H1 could be assigned unambiguously by standard peptide assignment procedure and, hence, the signal at 8.39 ppm could be attributed to the $H_{\epsilon 1}$ proton of H1 at pH 4.0. This signal evolves to 7.68 ppm if the pH is increased to 7.5 (data not shown).

In contrast, the assignment of the side chain resonances of the histidine residue at position two (H2) and four (H4) of the sequence of peptide 31, respectively, was not possible since the NH-backbone protons of these residues overlap. In order to identify the histidine residue which is involved in ZnO recognition ($H_{\epsilon 1}$ signal at 7.73; pH 7.5) the individual histidine residues were exchanged by alanine. Spectra in the presence and absence of ZnO were recorded for each mutant at pH 7.5 (Figure 6).

The chemical shifts of the $H_{\epsilon 1}$ signals of the three mutants (peptides 31_1, 31_2, and 31_4) do not coincide exactly with that one of peptide 31. However, regarding the spectra of mutant 31_2 in which H2 is exchanged by alanine it becomes obvious that one signal is broadened when ZnO was added, indicating that the Histidine residue which is involved in ZnO

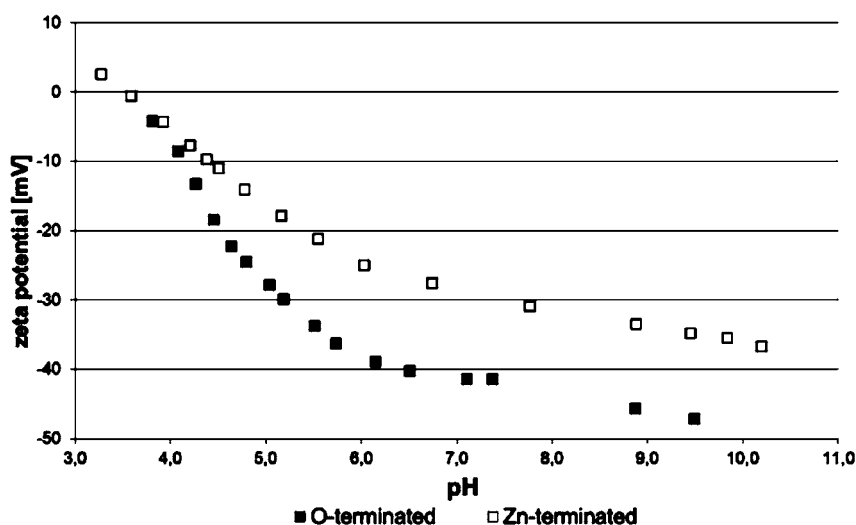


Figure 2. Zeta potential (ZP) of Zn- and O-terminated sides of single-crystalline ZnO (0001). For both sides the isoelectric point is around pH 3.5. The ZP of the oxygen-terminated side is lower than for the zinc-terminated side.

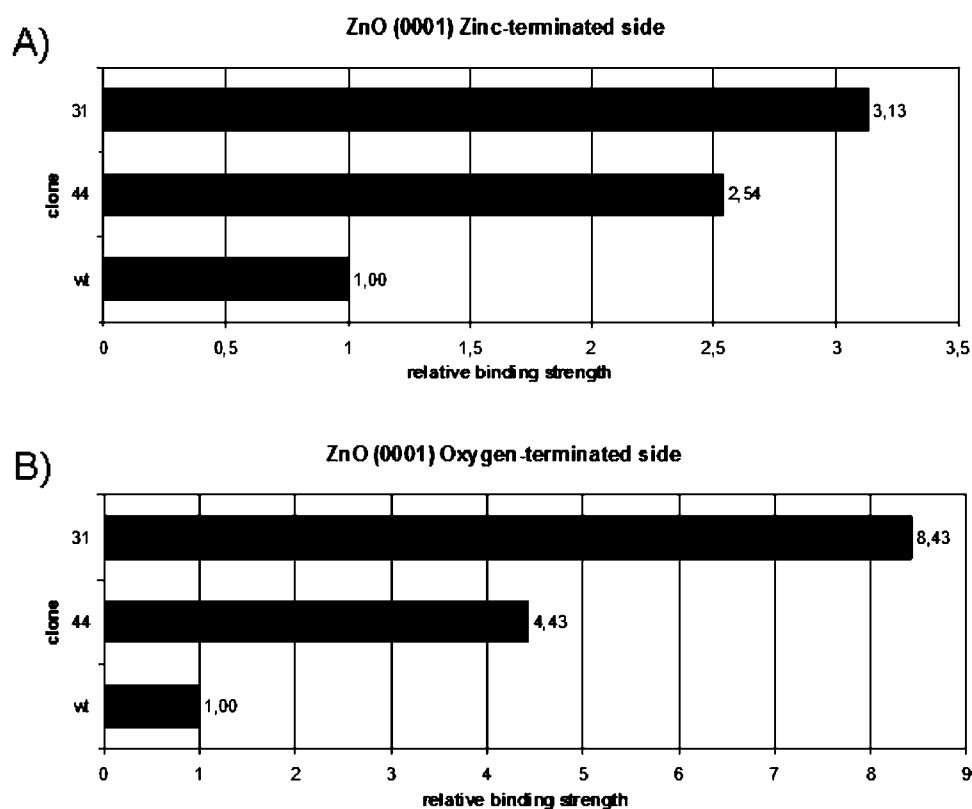


Figure 3. Binding strength of phage clones expressing peptide 31 and 44, respectively, to zinc- and oxygen-terminated side of ZnO substrate. The binding strength of phage clones at pH 7.5 was compared to the binding of wild-type (wt) phages expressing no additional peptide. Values were normalized to the binding strength of wt phage (wt = 1). (A) Binding strength to Zn-terminated side of single-crystalline ZnO (0001). (B) Binding strength O-terminated side of ZnO (0001).

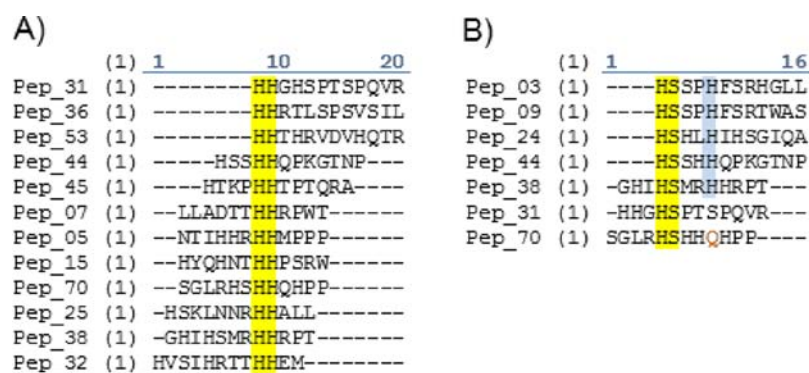


Figure 4. Sequence alignment of ZnO-binding peptides isolated from a randomized peptide library. (A) Combined alignment of peptides isolated from the Zn- and O-terminated side. Twelve out of 29 peptide sequences contain two neighboring histidine residues (HH, highlighted yellow). (B) Peptides isolated from O-terminated side of ZnO. The putative binding motive HSXXH was identified, which occurs at a frequency of approximately 1/3 (5 of 16) of the isolated peptides.

recognition is still present in the peptide mutant. Hence, H_{e1} of H4 is affected upon ZnO binding.

The affinities of peptides 31 and 44 to ZnO nanoparticles at pH 7.5 were determined by line broadening effects in NMR measurements at different ZnO concentrations ranging from 3 nM to 8 μ M (Figure 7). The signals of H4 H_{e1} (7.71 ppm) and H1 H_{e1} (7.73 ppm) protons were analyzed for peptide 31 and peptide 44, respectively. In order to allow the analysis of the data a 1:1 binding model was assumed. The affinity of peptide 31 was in the low nM range with a K_D value of 10 ± 3 nM. The K_D value of peptide 44 was determined at 260 ± 160 nM.

The binding of histidine to ZnO will lead to a shift of the histidine pK_a value suggesting a direct interaction of ZnO with histidine. The pK_a values of peptide 31 H4 H_{e1} and peptide 44 H1 H_{e1} protons in the absence and presence of ZnO nanoparticles were determined. 1D 1H NMR spectra in the pH range of 3.0–8.3 were recorded. The data were fitted to the Henderson–Hasselbalch equation,²⁶

$$\delta = [\delta_{\text{acid}} + \delta_{\text{base}} 10^{(\text{pH}-\text{pK}_a)}] / [1 + 10^{(\text{pH}-\text{pK}_a)}]$$

where δ is the chemical shift, and δ_{acid} and δ_{base} are the chemical shifts at the lowest and highest pH values, respectively. For

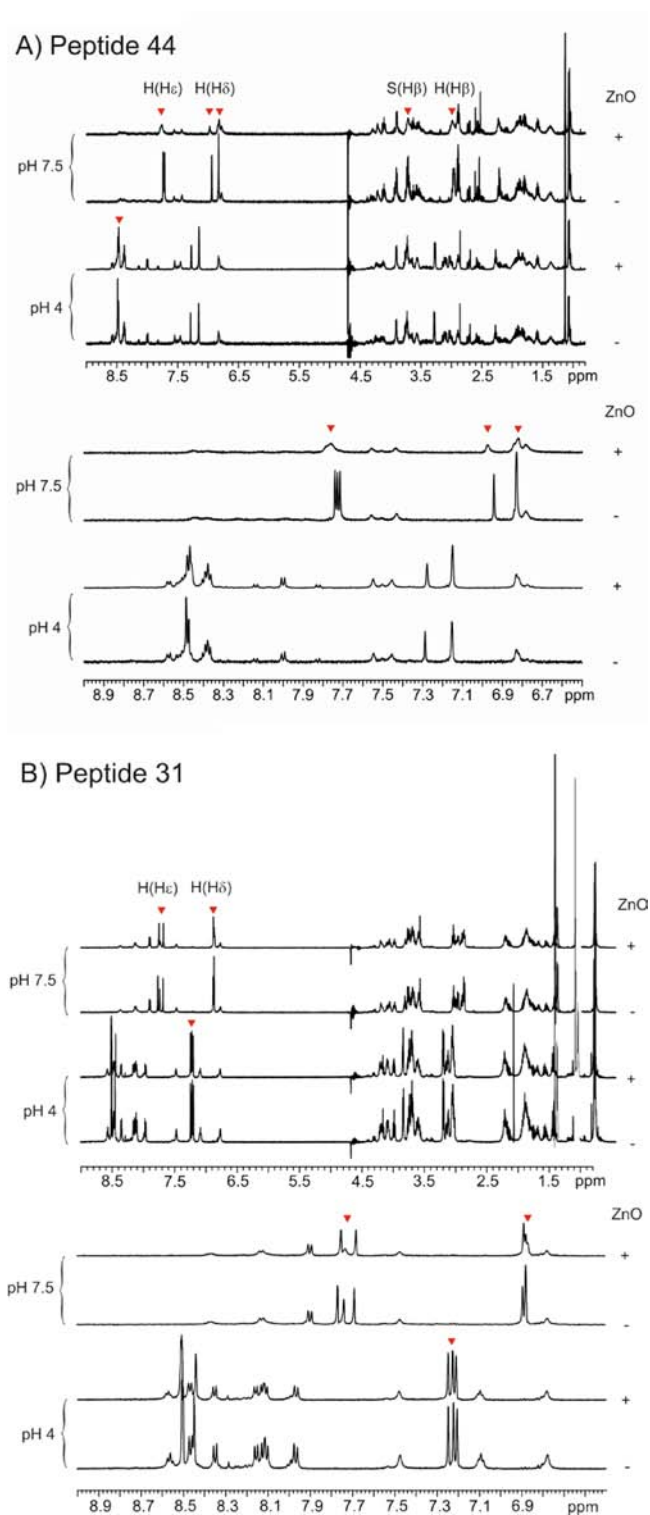


Figure 5. NMR spectra of peptide 44 (A) and 31 (B) in the absence and presence of ZnO nanoparticles. For each peptide the complete spectrum (0.8–9.0 ppm) and a magnification (6.5–9.0) is shown. Arrowheads indicate changes in the NMR signal intensities after adding ZnO nanoparticles. The binding amino acid residues and the interacting proton (in brackets) are indicated.

both peptides a shift of the pK_a to lower values was monitored due to ZnO binding (Table 3).

To address the question of the binding functionality of cysteine residues in ZnO-binding peptides serine was replaced

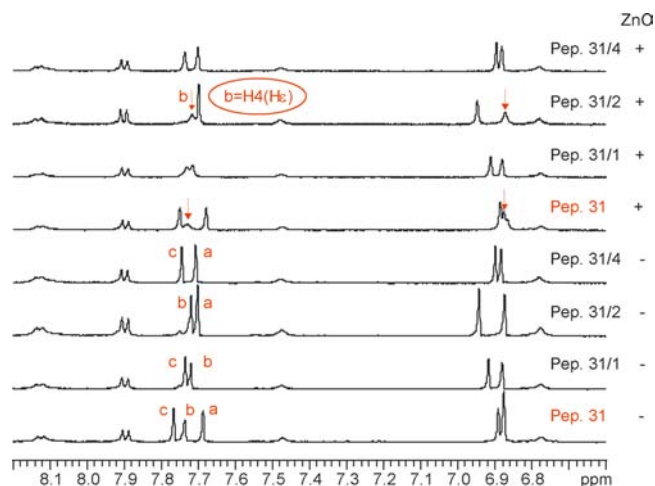


Figure 6. Alanine-scanning for the identification of the histidine residue in peptide 31, which interacts with ZnO nanoparticles. The individual histidine residues at position 1, 2, and 4 in peptide 31 were consecutively exchanged by alanine residues. By adding ZnO nanoparticles it was shown, that the histidine residues at position 4 (H4) is the binding partner.

by the structural analogue cysteine in the peptides 31 and 44, resulting in peptide 31Cys and 44Cys, respectively. The interaction sites on the molecular level were determined for both peptides (see Supporting Information for spectra and schematic drawing). First, the histidine residues of peptides 31Cys and 44Cys interacted similarly with ZnO like in the peptides containing serine. In addition, the H_{β} protons of all cysteine residues of peptides 31 and 44 showed line-broadening effects in the presence of ZnO.

DISCUSSION

Using the PD technique 29 different ZnO-binding peptides were isolated from a random peptide library.

Single-crystalline ZnO (0001) and (000-1), which were used as target substrates, have stable polar oxide surfaces.²⁷ The Zn-terminated and O-terminated surface sides exhibit different chemical and physical properties.²⁸ The ZPs for both sides were negative above pH 4, with a lower ZP of the O-terminated side compared to the Zn-terminated side ($\Delta ZP \approx 10$ mV at pH 7.5). ZPs of the single-crystalline ZnO substrate contrast the isoelectric points of ZnO powders, which are reported to vary between pH 7 and 10.²⁹ A significant deviation of the ZPs of single-crystalline substrates and powders are also known for other materials, like Al_2O_3 .³⁰ Additional charging mechanisms, like water structuring at the surface of the substrate and auto-proteolysis of interfacial water, were accounted for the low isoelectric point of single-crystal substrates.³⁰

The PD experiments revealed 13 and 10 peptide sequences, which bind exclusively to the zinc- and the oxygen-terminated side, respectively. In addition, six peptide sequences, which interact with the zinc- as well as the oxygen-terminated sides, were isolated. The enrichment in histidine residues in the isolated peptide pool was unambiguous (Table 2). Also, the accumulation of positively charged amino acid residues (lysine, arginine) within most of the peptides was striking. Since the Zn- and the O-terminated ZnO surface sides have a negative net charge at the pH of peptide screening (Figure 2), the binding of identical peptide sequences to both substrate sides is not astonishing. Positively charged arginine and lysine, were

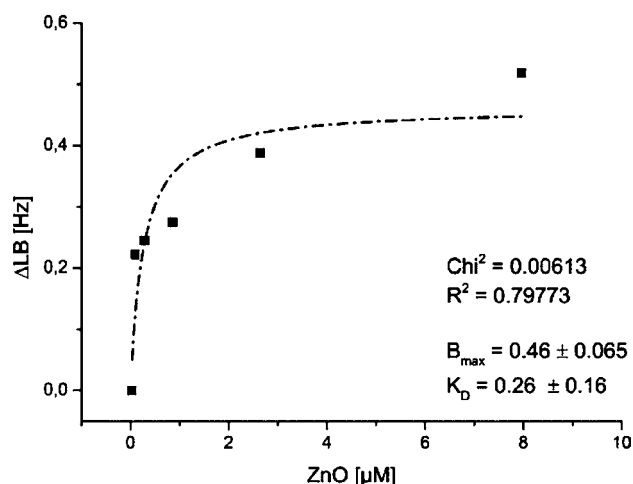
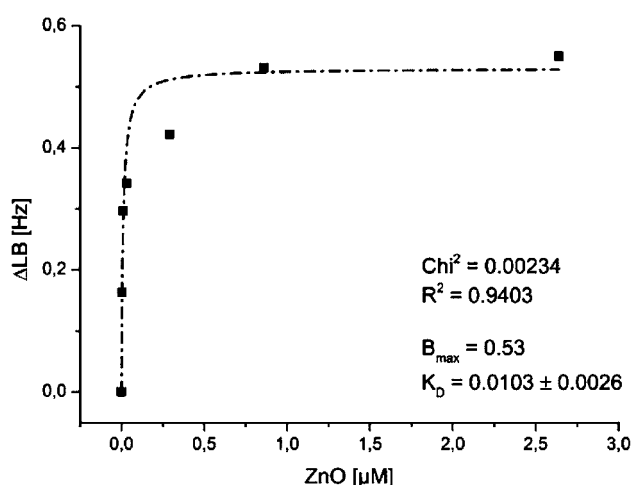
A) K_D peptide 44B) K_D peptide 31

Figure 7. Determination of the affinity (K_D value) of (A) peptide 44 and (B) peptide 31 to ZnO nanoparticles. NMR spectra were measured with increasing ZnO concentrations. Differences in line broadening versus ZnO concentration were plotted and the curve was fitted to one site binding model $y = B_{\max}x/(K_D + x)$. Both K_D values are in the nM range, with peptide 44 at 260 ± 160 nM and peptide 31 at 10 ± 3 nM.

overrepresented in peptides isolated from the Zn-terminated and the O-terminated side (approximately 50% higher frequency than in the initial peptide library). The result why these amino acids did not show signal changes due to ZnO

Table 3. pK_a Values of Peptides 31 and 44 in the Absence and Presence of ZnO Nanoparticles^a

	pK_a		ΔpK_a
	- ZnO	+ ZnO	
peptide 31	6.586	6.519	0.067
peptide 44	6.459	6.381	0.078

^aThe pK_a values of peptide 31 H4 ($H_{\epsilon 1}$) and peptide 44 H1 ($H_{\epsilon 1}$) were determined in the absence and presence of ZnO nanoparticles. Upon binding of histidine and ZnO the pK_a of the histidine residues become lower. The shift of the pK_a values is direct evidence for the histidine-ZnO binding.

binding in NMR spectroscopy may indicate that the interaction of the positively charged amino acid residues with ZnO is weaker than in the case of histidine, serine, and cysteine. For the inorganic-binding protein statherin, which binds to hydroxyapatite (HPA), the basic amino acids lysine and arginine were identified by solid state NMR to be involved in the interaction with HPA.^{31,32} Mineral crystal surfaces represent a mixture of anionic and cationic groups and therefore the interaction of negatively as well as positively charged amino acids in a peptide account for the binding.³³ Using sum frequency generation vibrational spectroscopy and quartz crystal microbalance measurements the structured binding of positively charged amino acids and peptides on inorganic oxide surface were determined.^{34–36} Also, positively charged lysine residues were identified for the interaction with SiO_2 in two different peptides.

Furthermore, the frequency of the negatively charged glutamic acid and aspartic acid were decreased compared to the native peptide library. The binding and repulsion of identical amino acid residues, based on ionic interactions of charged moieties, emphasize that the ZP of the inorganic substrate is negative for both sides.

The majority of ZnO-binding peptides have a high pI , resulting in peptides with a positive net charge at the pH of the experimental setup. About 60% of the peptides isolated from the O-terminated side, and thus significantly more than the peptides from the Zn-terminated side (37%), have a pI above pH 7.5, indicating that the binding of positively charged peptides (high pI values) is favored by a negatively charged substrate surface. In addition, the interaction of negatively charged (low pI values) or neutral peptides with the less negatively charged zinc-terminated side is comparably increased. Consequently, the fraction of negatively charged and neutral peptides, which bind to the zinc-terminated surface, is larger than the corresponding fraction binding to the oxygen-terminated one. This emphasize that ionic interactions of charged moieties have significant importance for the peptide binding to the target material.

The peptide sequences were aligned in order to identify a putative ZnO-binding motif based on conserved amino acid residues (Figure 4). The isolated peptide sequences are not an outcome of an evolutionary process, where diversification of an ancestor sequence occurs, but were identified within a combinatorial approach of peptide selection from a random library. Therefore, the relative position of the amino acid residues to each other is of greater significance than their absolute position within the sequence. Accordingly, the sequences were positioned relative to each other, regardless of a common starting point (e.g., N-terminus). For the oxygen-terminated side the putative binding sequence HSXXH was identified. The functional correlation of histidine and serine residues was confirmed by the NMR results, clearly showing the interaction of histidine and serine with ZnO nanoparticles.

The metal ion binding sites in zinc-dependent proteins are composed of histidine and/or cysteine residues.³⁷ Both amino acid residues directly interact with divalent zinc ions. In addition, the second-shell ligands aspartic acid and glutamic acid, which interact either directly or indirectly with Zn^{2+} ions, stabilize the metal ion binding.³⁷ Moreover, serine and threonine can substitute the stabilization function of aspartic acid and glutamic acid in proteins.³⁸ The electron affine zinc ions act as a Lewis acid binding to the nitrogen atoms of the imidazole ring of histidine, which is the electron pair donor.³⁹

Table 4. Enriched and Depleted Amino Acids in ZnO-Binding Peptides Identified by Phage Display Experiments

target substrate	method	pH	enriched amino acids	depleted amino acids	no. of sequences	publication
ZnO powder	PD	7.5	H/R, basic aa	Hydrophobic aa	5	Umetsu, 2005
ZnO powder	PD	7.5	Basic aa	n.d.	1	Tomczak, 2009
ZnO Zn-terminated	PD	7.5	H/K/D/G/A/S/L	Y/P/V/E/N/T	19	this work
ZnO O-terminated	PD	7.5	H/R	Y/V/E/D/K/A/I/L/F/Q	16	this work

Contrasting natural Zn-depending proteins, where the binding sites often contain cysteine residues, the isolated ZnO-binding peptide sequences lack cysteine residues. The absence of cysteine residues in the isolated peptides most probably does not reflect that cysteine did not bind to inorganic ZnO substrates in the experimental setup. More likely, the expression of cysteine residues may interfere with the life cycle of bacteriophages. Cysteine residues in peptide sequences interfere with the infectivity of phage clones and the secretion of pIII fusion proteins, respectively.^{40,41} Therefore, phage clones expressing peptides containing cysteine residues might be underrepresented in the isolated peptide pool. This is supported by the binding of the peptides 31Cys and 44Cys, where serine residues are exchanged by cysteine residues, to ZnO nanoparticles. Beside histidine also cysteine residues contribute to the interaction with ZnO nanoparticles. This emphasizes that the underrepresentation of cysteine residues in the isolated ZnO-binding peptides is rather due to biological restrictions than to the absent binding capacity of cysteine. Based on these findings inorganic-binding peptides identified by PD can be subsequently modified by serine to cysteine exchanges. For peptide 31Cys additional binding sites were generated by this modification which most probably influences the affinity of the peptide to the substrate.

The published peptide sequences isolated from ZnO powders by PD showed an enrichment of the basic amino acids histidine and arginine (Table 4),^{12,13} which was also shown using a CSD experimental setup.¹¹ Our work clearly confirms the enrichment of histidine residues in ZnO-binding peptides and show that the increased histidine content is not limited to one side of the polar substrate, but was observed for the Zn- as well as the O-terminated side.

CSD experiments also showed the enrichment of aspartic acid and arginine.¹¹ In this study it was specified that the negatively charged aspartic acid was overrepresented in peptides from the Zn-terminated side and the positively charged arginine was enriched for peptides isolated from the O-terminated side. With this study, the enrichment of aspartic acid and arginine can be explained and specified. The Zn-terminated side is less negative than the O-terminated side and hence less repellent for aspartic acid but also less attractive for arginine. For the more negatively charged O-terminated side the interaction with arginine is favored while the interaction with aspartic acid is restrained.

Peptides lacking histidine residues were also isolated using PD (Table 1), suggesting that there are other important amino acid residues for the peptide-ZnO binding. The seven peptide sequences (06, 20, 21, 26, 29, 46, and 52) were more heterogeneous compared to histidine-containing peptides. The peptides were almost exclusively isolated from the Zn-terminated substrate side and the average $pI = 6.8$ of non-histidine-containing peptides was clearly below the average $pI = 8.5$ of the complete pool of isolated peptide sequences. Within these seven peptides the content of tryptophan, glycine and methionine was roughly doubled compared to an unchallenged

peptide library. In contrast, the number of threonine, valine, tyrosine, and glutamate was decreased. Thai et al.,¹⁰ who isolated a set of ZnO-binding peptides which were lacking of histidine residues, also reported an increase in tryptophan and glycine and a depletion of tyrosine residues. However, it was not specified whether the peptides bind to the Zn- or the O-terminated substrate side. At the experimental conditions of peptide isolation only lysine, arginine, aspartic acid, glutamic acid, and the peptide termini have charged moieties. From the finding that the remaining uncharged or polarized amino acid residues were enriched for one side and depleted for the other, it can be inferred that beside ionic interactions of charged atoms, interactions of nonionic moieties contribute to the binding. The molecular interactions of the two most abundant peptides (31 and 44) were analyzed by means of NMR spectroscopy using chemical shift perturbations and line-broadening effects to determine the interaction of C-bound protons of the peptides with ZnO nanoparticles. Histidine and serine residues were clearly identified as binding partner for ZnO nanoparticles. Furthermore, the pK_a shifts of histidine residues in peptides 31 and 44 in the presence of ZnO emphasize the involvement of histidine in the binding. Also a clear pH dependency of the binding was shown. The binding event is strongly affected by the peptide charge (reflected by pK_a , the protonation of the amino acid side chains and the peptide termini), which is mainly dependent on the pH of the solution. In addition, the electrostatic parameters are influenced by the primary peptide sequence, because the microenvironment induced by neighboring amino acid residues has an influence on the properties of individual amino acid residues of the peptide. The experimental setup avoids the detection of peptide-peptide interactions, since changes in NMR spectrum of peptides with ZnO compared to the spectrum of peptides only were analyzed. Possible inter-peptide interactions are detected in both NMR spectra and thus will not to inter-spectrum changes. Therefore, peptide-peptide interactions are not included in the determination of binding sites. Peptide 44 showed a pronounced pH dependency of the ZnO binding. At pH 4.0 only the first histidine residue (H1) in the peptide sequence showed a binding effect. At this pH histidine is protonated and harbors a positive charge. At pH 7.5, which was used for the PD experiments, all histidine and serine residues, which have no charge at this pH, were assigned for the interaction with ZnO nanoparticles in solution. This shows that besides ionic interactions of charged molecules, the uncharged histidine and serine residues bind to ZnO nanoparticles, too. The binding events of the uncharged amino acid residues might be attributed to nonionic interactions of polarized moieties.

On the atomic level the numbers of potential binding sites of individual histidine residues were increased from only one at pH 4.0 to three interaction sites at pH 7.5 (Figure 8A). At pH 7.5 the imidazole ring of histidine ($pK_a = 6.0^{42}$) is supposed to be uncharged. The uncharged imidazole ring might reduce the ionic repulsion of positively charged ZnO nanoparticles ($pI = 9.5$)⁴³ and facilitate binding to ZnO. With decreasing pH

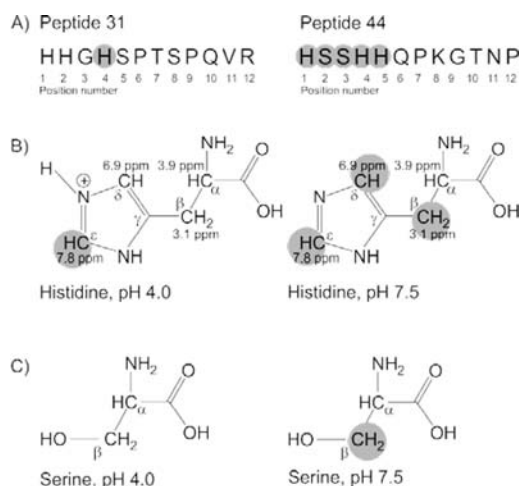


Figure 8. Scheme of the interaction sites between amino acids and ZnO nanoparticles on the peptide and atomic levels. (A) Interacting amino acid residues in peptides 31 and 44. The interaction sites of the peptides at pH 7.5 are highlighted in gray. Position numbers of the amino acid residues in the peptides are given below the sequences. (B) Interacting H-atoms of histidine showed a pronounced pH dependency, which can be attributed to the charge states of histidine ($pK_a = 6.0$) at various pH values. At pH 4.0, H_{e1} interacted with ZnO, while at pH 7.5, three interacting H atoms (H_{e1} , $H_{\delta1}$, and H_{β}) were detected by NMR. (C) H_{β} of serine in peptide 44 interacts with ZnO nanoparticles only at pH 7.5. This interaction also shows a pH dependency, despite the constant charge state of serine over the investigated pH range ($pK_a \approx 16$).

values, the histidine residues become positively charged and the repulsion of the positively charged ZnO nanoparticles increases. At pH 4.0, only the H_{e1} proton peak of histidine showed a line-broadening effect, which can be attributed to the binding of ZnO nanoparticles to the charged imidazole ring. The line-broadening effects are observed for the C-bound protons. Presumably, this effect is based on the close proximity of these protons to the chemically favored interaction site of the ZnO nanoparticles with the nitrogen atoms of the imidazole ring. A similar effect was observed at the interaction of the serine C_{β} protons with ZnO nanoparticles. Due to the polarized character of serine hydroxyl groups, they are favored for electrostatic interactions with ZnO nanoparticles as in the above-mentioned case. Because of the vicinity of the H_{β} protons and the hydroxyl group, the chemical environment of the H_{β} protons will be affected by the ZnO binding, resulting in the observed significant line-broadening effects of H_{β} protons. With increasing pH the polarity of the hydroxyl group increases, which favors ZnO binding at pH 7.5. The corresponding H_{β} protons in the structural analogue cysteine showed changes in NMR signals in the presence of ZnO, too. The same effect of the serine OH group is assumed for the SH group of the cysteine residues.

The affinities of both ZnO-binding peptides to the substrate at pH 7.5 were determined in the nanomolar range (peptide 31, $K_D = 10 \pm 3$ nM; peptide 44, $K_D = 260 \pm 160$ nM). The results show a clear trend that peptide 31 binds more strongly to the substrate than peptide 44. However, it should be stated that, for a more precise comparison of the affinities, further NMR competition experiments should be taken into account. The peptide affinities are in accordance with the binding of peptide–phage entities to ZnO, showing a higher binding strength for phages expressing peptide 31 compared to phages

with peptide 44. High affinities of inorganic binding peptides to their substrate with K_D values in the low nanomolar range were reported for other peptides binding to gold⁴⁴ and titanium dioxide.⁴⁵ For peptide 31, the binding to ZnO nanoparticles was detected only at pH 7.5 using NMR spectroscopy. Surprisingly, only the histidine at position four of the peptide sequence showed a clear interaction with ZnO. In contrast to peptide 44, where all serine residues contribute to the binding, in peptide 31 none of the serine residues were assigned for binding. This corroborates the assumption that the micro-environment, determined by the primary peptide sequence, influences the binding efficiency of single amino acids. In peptide 44, the directly neighboring amino acids of serine were only histidine residues, while for peptide 31, besides histidine, proline and threonine are flanking the serine residue. Serine also showed a pH-dependent binding behavior (Figure 8B), although the charge state of serine is constant over the investigated pH range (pK_a of serine ~ 16). This, once more, emphasized that nonionic interactions influence the binding. Different binding characteristics were also monitored for histidine residues. For peptide 44, the electronegative oxygen atoms of the serine residues may induce the binding of histidine to ZnO at pH 7.5, e.g. by charge displacement, hydrogen atoms shifting, or weak intramolecular forces like polar interactions, hydrogen bonding, or van der Waals forces. With increasing positive charges of the histidine residues converging at pH 4.0, these weak interactions might become negligible facing strong charge effects, and the four binding sites in histidine at pH 7.5 are reduced to only one residual at pH 4.0.

Besides the primary peptide sequence the conformation and hence steric effects may also influence the binding capacity.⁴⁶ Therefore, the N-terminal histidine residues of peptide 31 and peptide 44 might interact differently with ZnO nanoparticles.

CONCLUSION

In this report the phage display technique and NMR spectroscopy were combined for the identification of binding sites at the atomic level of peptides, which interact specifically with single-crystalline ZnO substrates.

The pI and thus the charge state of the isolated peptides play a major role for the ionic interactions of the organic and inorganic components. Peptides with a low pI interact more strongly with the ZnO side with a higher zeta potential (less negatively charged surface), and peptides with a high pI interact more strongly with the substrate side with a lower ZP (more negatively charged). NMR investigations were applied for the identification of nonionic interactions of amino acid residues and ZnO nanoparticles. It was confirmed that polar interactions of nonionic amino acid residues also play an important role in the binding to inorganic materials. The amino acids predicted to form the ZnO-binding epitope (histidine and serine) by sequence alignment were experimentally confirmed. In addition, the pH dependency of the peptide–ZnO interaction was shown by NMR. The isolation of inorganic-binding peptides with high affinity to their substrates with K_D values in the nanomolar range favors their applications in various technical fields. Based on the information of increased and depleted amino acid residues of peptides lacking histidine residues, artificial ZnO-binding peptides with no natural protein parallels can be generated.

The approach of combined PD and NMR can be generalized for the determination of binding epitopes for other peptide–inorganic substrate combinations for target-oriented tailoring

and design of peptides for applications in, e.g., surface functionalization or biomineralization processes.

■ ASSOCIATED CONTENT

📄 Supporting Information

Schematic drawing of the PD method and expansion of the TOCSY and ROESY spectra of peptides 31 and 44, with tables of the associated ^1H shifts; diagrams of pK_a value determinations; peptides 31Cys and 44Cys 1D ^1H NMR spectra and tables of the associated ^1H shifts as well as a schematic drawing of binding sites at the molecular level of cysteine residues. This material is available free of charge via the Internet at <http://pubs.acs.org>.

■ AUTHOR INFORMATION

Corresponding Author

dirk.rothenstein@imw.uni-stuttgart.de

Present Address

[†]Institute for Physical Chemistry, University of Stuttgart, Pfaffenwaldring 55, 70569 Stuttgart, Germany

Notes

The authors declare no competing financial interest.

■ ACKNOWLEDGMENTS

The financial support of DFG (BI469/15-1) within the scope of the project "Biologische Erzeugung von Oxidkeramiken" (PAK 440) is gratefully acknowledged.

■ REFERENCES

- (1) McAlpine, M. C.; Agnew, H. D.; Rohde, R. D.; Blanco, M.; Ahmad, H.; Stuparu, A. D.; Goddard, W. A.; Heath, J. R. *J. Am. Chem. Soc.* **2008**, *130*, 9583.
- (2) Kuang, Z.; Kim, S. N.; Crookes-Goodson, W. J.; Farmer, B. L.; Naik, R. R. *ACS Nano* **2009**, *4*, 452.
- (3) de Jonge, L.; Leeuwenburgh, S.; Wolke, J.; Jansen, J. *Pharm. Res.* **2008**, *25*, 2357.
- (4) Xing, Z.-C.; Chang, Y.; Kang, I.-K. *Sci. Technol. Adv. Mater.* **2010**, *11*, 014101.
- (5) Tamerler, C.; Sarikaya, M. *Acta Biomater.* **2007**, *3*, 289.
- (6) Gao, P. X.; Wang, Z. L. *J. Appl. Phys.* **2005**, *97*.
- (7) Gerstel, P.; Hoffmann, R. C.; Lipowsky, P.; Jeurgens, L. P. H.; Bill, J.; Aldinger, F. *Chem. Mater.* **2006**, *18*, 179.
- (8) Gerstel, P.; Lipowsky, P.; Durupthy, O.; Hoffmann, R. C.; Bellina, P.; Bill, J.; Aldinger, F. *J. Ceram. Soc. Jpn.* **2006**, *114*, 911.
- (9) Bauermann, L. P.; del Campo, A.; Bill, J.; Aldinger, F. *Chem. Mater.* **2006**, *18*, 2016.
- (10) Thai, C. K.; Dai, H. X.; Sastry, M. S. R.; Sarikaya, M.; Schwartz, D. T.; Baneyx, F. *Biotechnol. Bioeng.* **2004**, *87*, 129.
- (11) Kjaergaard, K.; Sorensen, J. K.; Schembri, M. A.; Klemm, P. *Appl. Environ. Microbiol.* **2000**, *66*, 10.
- (12) Tomczak, M. M.; Gupta, M. K.; Drummy, L. F.; Rozenzhak, S. M.; Nalk, R. R. *Acta Biomater.* **2009**, *5*, 876.
- (13) Umetsu, M.; Mizuta, M.; Tsumoto, K.; Ohara, S.; Takami, S.; Watanabe, H.; Kumagai, I.; Adschiri, T. *Adv. Mater.* **2005**, *17*, 2571.
- (14) Naik, R. R.; Brott, L. L.; Clarson, S. J.; Stone, M. O. *J. Nanosci. Nanotechnol.* **2002**, *2*, 95.
- (15) Dickerson, M. B.; Sandhage, K. H.; Naik, R. R. *Chem. Rev.* **2008**, *108*, 4935.
- (16) Brown, S. *Nat. Biotechnol.* **1997**, *15*, 269.
- (17) Naik, R. R.; Stringer, S. J.; Agarwal, G.; Jones, S. E.; Stone, M. O. *Nat. Mater.* **2002**, *1*, 169.
- (18) Heinz, H.; Farmer, B. L.; Pandey, R. B.; Slocik, J. M.; Patnaik, S. S.; Pachter, R.; Naik, R. R. *J. Am. Chem. Soc.* **2009**, *131*, 9704.
- (19) Lee, S. W.; Mao, C. B.; Flynn, C. E.; Belcher, A. M. *Science* **2002**, *296*, 892.

- (20) Flynn, C. E.; Mao, C. B.; Hayhurst, A.; Williams, J. L.; Georgiou, G.; Iverson, B.; Belcher, A. M. *J. Mater. Chem.* **2003**, *13*, 2414.
- (21) Costa, D.; Irrera, S.; Mucus, P. *J. Mol. Struct.: Theochem.* **2009**, *903*, 49.
- (22) Idriss, H.; Gao, Y. K.; Traeger, F.; Shekhah, O.; Woll, C. J. *Colloid Interface Sci.* **2009**, *338*, 16.
- (23) Ganguly, T.; Mandal, G.; Bhattacharya, S. *Chem. Phys. Lett.* **2009**, *472*, 128.
- (24) Patwardhan, S. V.; Patwardhan, G.; Perry, C. C. *J. Mater. Chem.* **2007**, *17*, 2875.
- (25) Rabung, T.; Schild, D.; Geckeis, H.; Klenze, R.; Fanghanel, T. *J. Phys. Chem. B* **2004**, *108*, 17160.
- (26) Dai, Q.; Lea, C. R.; Lu, J.; Piccirilli, J. A. *Org. Lett.* **2007**, *9*, 3057.
- (27) Wander, A.; Harrison, N. M. *J. Chem. Phys.* **2001**, *115*, 2312.
- (28) Vohs, J. M.; Barteau, M. A. *Surf. Sci.* **1986**, *176*, 91.
- (29) Kosmulski, M. *Chemical properties of material surfaces*; Marcel Dekker: 2001.
- (30) Lützenkirchen, J.; Zimmermann, R.; Preocanin, T.; Filby, A.; Kupcik, T.; Kuttner, D.; Abdelmonem, A.; Schild, D.; Rabung, T.; Plaschke, M.; Brandenstein, F.; Werner, C.; Geckeis, H. *Adv. Colloid Interface* **2010**, *157*, 61.
- (31) Gibson, J. M.; Raghunathan, V.; Popham, J. M.; Stayton, P. S.; Drobny, G. P. *J. Am. Chem. Soc.* **2005**, *127*, 9350.
- (32) Ndao, M.; Ash, J. T.; Stayton, P. S.; Drobny, G. P. *Surf. Sci.* **2010**, *604*, L39.
- (33) Duer, M. J. *Surf. Sci.* **2010**, *604*, 1237.
- (34) York, R. L.; Holinga, G. J.; Somorjai, G. A. *Langmuir* **2009**, *25*, 9369.
- (35) York, R. L.; Mermut, O.; Phillips, D. C.; McCrea, K. R.; Ward, R. S.; Somorjai, G. A. *J. Phys. Chem. C* **2007**, *111*, 8866.
- (36) Mermut, O.; Phillips, D. C.; York, R. L.; McCrea, K. R.; Ward, R. S.; Somorjai, G. A. *J. Am. Chem. Soc.* **2006**, *128*, 3598.
- (37) Maret, W.; Li, Y. *Chem. Rev.* **2009**, *109*, 4682.
- (38) Dudev, T.; Lim, C. *Chem. Rev.* **2003**, *103*, 773.
- (39) Lin, Y.-L.; Lim, C. *J. Am. Chem. Soc.* **2004**, *126*, 2602.
- (40) Kay, B. K.; Adey, N. B.; He, Y. S.; Manfredi, J. P.; Mataragnon, A. H.; Fowlkes, D. M. *Gene* **1993**, *128*, 59.
- (41) Peters, E. A.; Schatz, P. J.; Johnson, S. S.; Dower, W. J. *J. Bacteriol.* **1994**, *176*, 4296.
- (42) Berg, J. M.; Tymoczko, J. L.; Stryer, L. *Biochemistry*, 6th ed.; W.H. Freeman: New York, 2007.
- (43) Ostomel, T. A.; Shi, Q.; Stoimenov, P. K.; Stucky, G. D. *Langmuir* **2007**, *23*, 11233.
- (44) Tamerler, C.; Duman, M.; Oren, E. E.; Gungormus, M.; Xiong, X. R.; Kacar, T.; Parviz, B. A.; Sarikaya, M. *Small* **2006**, *2*, 1372.
- (45) Gronewold, T. M. A.; Baumgartner, A.; Weckmann, A.; Knekties, J.; Egler, C. *Acta Biomater.* **2009**, *5*, 794.
- (46) Kantarci, N.; Tamerler, C.; Sarikaya, M.; Haliloglu, T.; Doruker, P. *Polymer* **2005**, *46*, 4307.